Biomass and Bioenergy 187 (2024) 107301

Contents lists available at ScienceDirect

Biomass and Bioenergy

journal homepage: www.elsevier.com/locate/biombioe

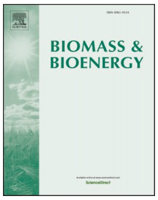

Interaction of furfural and hexadecane as bio-oil and plastics pyro-oil model compounds with non-thermal plasma processing as a route to *in-situ* hydrogen donor upgrading of bio-oil

Maryam Khatibi, Mohamad A. Nahil, Paul T. Williams *

School of Chemical & Process Engineering, University of Leeds, Leeds, LS2 9JT, UK

A R T I C L E   I N F O

Keywords:
Biomass
Waste plastics: hydrogen donor
Non-thermal plasma

A B S T R A C T

Bio-oil upgrading by deoxygenation with a hydrogen donor has been investigated using a model bio-oil compound (furfural) and a model hydrocarbon (hexadecane) typically produced from plastics pyrolysis as the hydrogen donor. Upgrading has been investigated using a non-thermal plasma reactor system with the presence of hexadecane to improve bio-oil quality by raising the H/C ratio. The effect of input power on product yield, oil and gas composition has been investigated. There was little synergistic interaction between furfural and hexadecane in the absence of plasma. However, introduction of the non-thermal plasma, and increasing the input power for the furfural: hexadecane mixture resulted in a greater yield of gas components, along with the production of single ring aromatic and mono-oxygenated oil compounds, while dual-oxygenated compounds in the oil were reduced. There was a positive synergy for most light hydrocarbons, with higher input plasma power leading to higher positive synergy percentages. Conversely, the synergistic effect for most heavy hydrocarbons was negative, suppressing the formation of higher molecular weight oil compounds, which intensified with higher input plasma power levels. This phenomenon may be attributed to high-energy electrons in the non-thermal plasma environment colliding with volatile components of the feedstock, aiding in deoxygenation and the production of light hydrocarbons.

1. Introduction

The transition towards renewable energy sources is imperative considering the finite nature of fossil fuels and their adverse environmental impact during use [1,2]. Biomass-derived biofuels present a promising avenue for meeting energy demands sustainably. Not only do they offer a renewable alternative to fossil fuels, but they also contribute to mitigating atmospheric pollution and fostering rural development [3]. Embracing renewable and sustainable fuels can lead towards a more environmentally friendly and socially equitable energy future [2]. The utilization of biomass, as the sole carbon-bearing renewable energy source, is essential for achieving environmental and energy sustainability, as well as carbon neutrality goals. The thermochemical processing of biomass through pyrolysis, gasification or combustion holds the potential to make substantial contributions to all three key energy sectors: transport, heat, and electricity [4–6].

The pyrolysis of biomass produces a mainly bio-oil product with oil yields of up to 70 wt% in addition to the production of char and gas [2–4]. The bio-oil has been proposed as a renewable liquid fuel and as a viable alternative to petro-crude oil [3]. However, the primary drawbacks of bio-oils obtained from pyrolysis include poor quality attributed to the presence of a high content of oxygenated compounds, high moisture content, high viscosity, storage instability, low heating value, and acidity [7–10]. It has been proposed that pathways from biomass pyrolysis bio-oil to transportation fuels becomes economically sustainable only when the bio-oil is upgraded to enhance its physicochemical properties [10,11]. Bio-oil upgrading to enable the direct substitution of upgraded bio-oils into the existing petroleum refinery infrastructure, as a ‘drop-in’ bio-oil is highly desirable since it enables usage of the existing petroleum refinery infrastructure and would support the long-term sustainability of biomass-to-fuels technology. The bio-oil derived from various biomass feedstocks typically comprises hundreds of organic compounds, significantly complicating the investigation of new process developments, catalytic activities and reaction pathways involved in the upgrading process. Therefore, in order to understand the complex process of bio-oil upgrading numerous studies have used model bio-oil

---

* Corresponding author.
E-mail address: p.t.williams@leeds.ac.uk (P.T. Williams).

https://doi.org/10.1016/j.biombioe.2024.107301
Received 8 May 2024; Received in revised form 20 June 2024; Accepted 30 June 2024

compounds such as furfural, anisole, methanol and guaiacol, which serve as representative compounds of biomass pyrolysis oils [12–15]. In this work, furfural has been used as the representative model bio-oil compound, since it has been used in other studies as a pyrolysis bio-oil model compound [14,15] and is found in significant concentrations in pyrolysis bio-oil [16,17].

Methods to address the drawbacks and enhance the qualities of bio-oils can be categorized into *ex-situ* and *in-situ* processes [18]. Among these, *in-situ* processes are considered simpler, more efficient, and lower-cost techniques for producing drop-in fuels [18]. *In-situ* application of hydrogen donors to the bio-oil upgrading process by deoxygenation of the bio-oil have been proposed. Hydrogen donors must be capable of releasing hydrogen in an activated state to the reaction system, enabling transfer of hydrogen from the donor compound to the acceptor compound and thereby, enhance hydrodeoxygenation of the pyrolysis bio-oil. For example, liquid phase hydrogen donors such as tetralin, (a naphtheno-aromatic compound of crude petroleum oil), have been used to donate hydrogen for saturating the cracking products from cellulose to produce high yield liquid hydrocarbons with a very low content of oxygenated compounds [19]. In addition, *in-situ* generated H_2 was proposed for bio-oil upgrading over platinum catalysts [20], it was suggested that *in-situ* H_2 was generated initially from the reforming of light oxygenates, which then promoted the scission of C–O bonds. A recent novel development has been the introduction of co-pyrolysis of biomass and plastics for the upgrading of bio-oils, where the plastic polymers serve as hydrogen donors, thereby enhancing the H_2 transfer process and aiding in the deoxygenation of the product bio-oils [18,21]. Waste plastics thermally degrade to produce a range of hydrogen-rich hydrocarbons based principally on the polymer structure of the original plastic. Hydrogen and hydrogen-rich hydrocarbon gases/vapours and reactive hydrogen species generated from waste plastics pyrolysis have the potential to promote bio-oil deoxygenation through *in situ* hydrogenation and hydrogen transfer reactions. This method has been identified as one of the most promising in-situ procedures to improve the quality and stability of bio-oil [18,21]. In this work, hexadecane has been chosen as the model hydrocarbon compound to be investigated as a representative compound of plastic pyrolysis oil. Hexadecane has been identified in significant concentrations in the pyro-oil product from the pyrolysis of the common polyolefin plastics, high density polyethylene [22], low density polyethylene [23] and polypropylene [24]. Hexadecane has also been used as a representative model compound for studies into the cracking of heavy hydrocarbon oil [25,26].

Non-thermal plasma processing is a novel technique that has received high recent interest and is considered as a viable technique for bio-oil upgrading [7,13,27]. Non-thermal plasma offers an attractive alternative to the conventional catalytic route for upgrading bio-oils and can be achieved at atmospheric pressure and low temperatures ($<$250 °C). In non-thermal plasmas, the overall gas temperature is low, while the electrons are highly energetic with a typical electron temperature of 1–10 eV, which interact with the gas reactants in the plasma to produce a cascade of processes yielding a variety of chemically reactive species including free radicals, excited atoms, ions and molecules for the initiation of different physical and chemical reactions [20]. The non-equilibrium character of such plasma enable thermodynamically unfavourable reactions to occur at low temperatures. Non-thermal plasma technology has been reported as an effective alternative approach for upgrading bio-oil at low temperatures and atmospheric pressure [13]. Non-thermal plasma reactors include dielectric barrier discharge (DBD), gliding arc and corona type reactors. The DBD non-thermal plasma reactor has been used to upgrade and crack model bio-oil compounds, with the key aim of deoxygenation of the bio-oil as a step towards upgrading. For example, Taghvaei et al. [13], used a DBD plasma reactor to upgrade guaiacol as a representative lignin derived pyrolytic-oil model compound. They found that a guaiacol conversion of 81 % and a deoxygenation degree of 52 % were achieved without the use of any catalyst and hydrogen. Phenol was produced selectively through direct demethoxylation, but, no hydrogenation of the aromatic ring was observed due to operation at low temperature and atmospheric pressure. Saleem et al. [28], studied the decomposition of benzene as a biomass gasification tar model compound in a DBD reactor with CH_4 carrier gas. They reported that the breakdown of benzene increased as both input power and residence time was increased, the highest benzene decomposition reached 82.9 %. The primary gaseous by-products were H_2 and lower hydrocarbons, and their production also rose with increasing input power and residence time.

In summary, two complimentary routes for bio-oil upgrading via deoxygenation are identified, (i) co-pyrolysis of biomass and plastics through hydrogen donation from the plastics to the bio-oil and (ii) the additional process of non-thermal plasma to enhance the hydrogen donor deoxygenation process. However, to the authors knowledge, there are no reports investigating this simultaneous dual approach of deoxygenation of bio-oil. In this report, we have investigated the interaction of a model bio-oil compound (furfural) and a model hydrocarbon compound (hexadecane) representative of plastics pyrolysis oil acting in the role of a hydrogen donor. The interaction was investigated using a DBD non-thermal plasma reactor system over a range of input plasma powers in relation to the detailed composition of the product gas and bio-oil.

2. Materials and methods

2.1. Materials

Furfural (furan-2-carbaldehyde) was chosen as the model representative oxygenated bio-oil compound with a chemical formula of $C_5H_4O_2$. The properties of furfural are, molar mass, 96.085 g mol^{-1}, density, 1.1601 g mL^{-1} and boiling point 162 °C. Hexadecane was chosen as the model representative hydrocarbon found in pyrolysis oils derived from the pyrolysis of polyolefin plastics with a chemical formula $C_{16}H_{34}$. The properties of hexadecane are, molar mass, 224.448 g mol^{-1}, density, 0.77 g mL^{-1} and boiling point 286 °C. The furfural and hexadecane were obtained from Merck, Darmstadt, Germany.

2.2. Experimental reactor system

Experiments were undertaken using a two-stage, vaporisation-non-thermal plasma reactor system, illustrated in Fig. 1. In the first stage, vaporisation of the model compound furfural and/or hexadecane feedstock was carried out. The vaporisation reactor (250 mm length and 20 mm internal diameter) was filled with stainless steel packing to increase the surface area and held at a temperature of 300 °C. Furfural and/or hexadecane with a purity of 99 % were introduced into the reactor as liquid feed using two HPLC pumps (SPLG100) with a flow rate of 5 ml/h furfural or hexadecane. The resulting vapours were then transferred directly to a second-stage dielectric barrier discharge non-thermal plasma reactor for plasma upgrading. Nitrogen served as the purge carrier gas with a flow rate of 50 ml min^{-1}. An electric ceramic insulator connecting tube separated the vaporisation and plasma reactors. The second-stage DBD non-thermal plasma reactor was constructed of quartz glass with a 23 mm diameter and was held at a temperature of 250 °C. It was a coaxial DBD plasma reactor, consisting of two electrodes as shown in Fig. 2. The inner stainless-steel electrode, 254 mm in length and 18 mm in diameter, was connected to the power supply and located in the middle of the reactor. The outer electrode was a 95 mm long copper mesh used as the low-voltage electrode, wrapped around a quartz glass tube. The quartz tube acted as a dielectric material, separating the inner and outer electrodes. The discharge zone, where plasma reactions occurred, was the region between the two electrodes with a 95 mm axial length and a discharge gap of 5 mm. The product gases were collected in the gas sample bag for a time period of 35 min for analysis using gas chromatography (GC). The liquid products were collected from the condensers at the end of each experiment using dichloromethane solvent and then analyzed by gas chromatography–mass spectrometry (GC–MS).

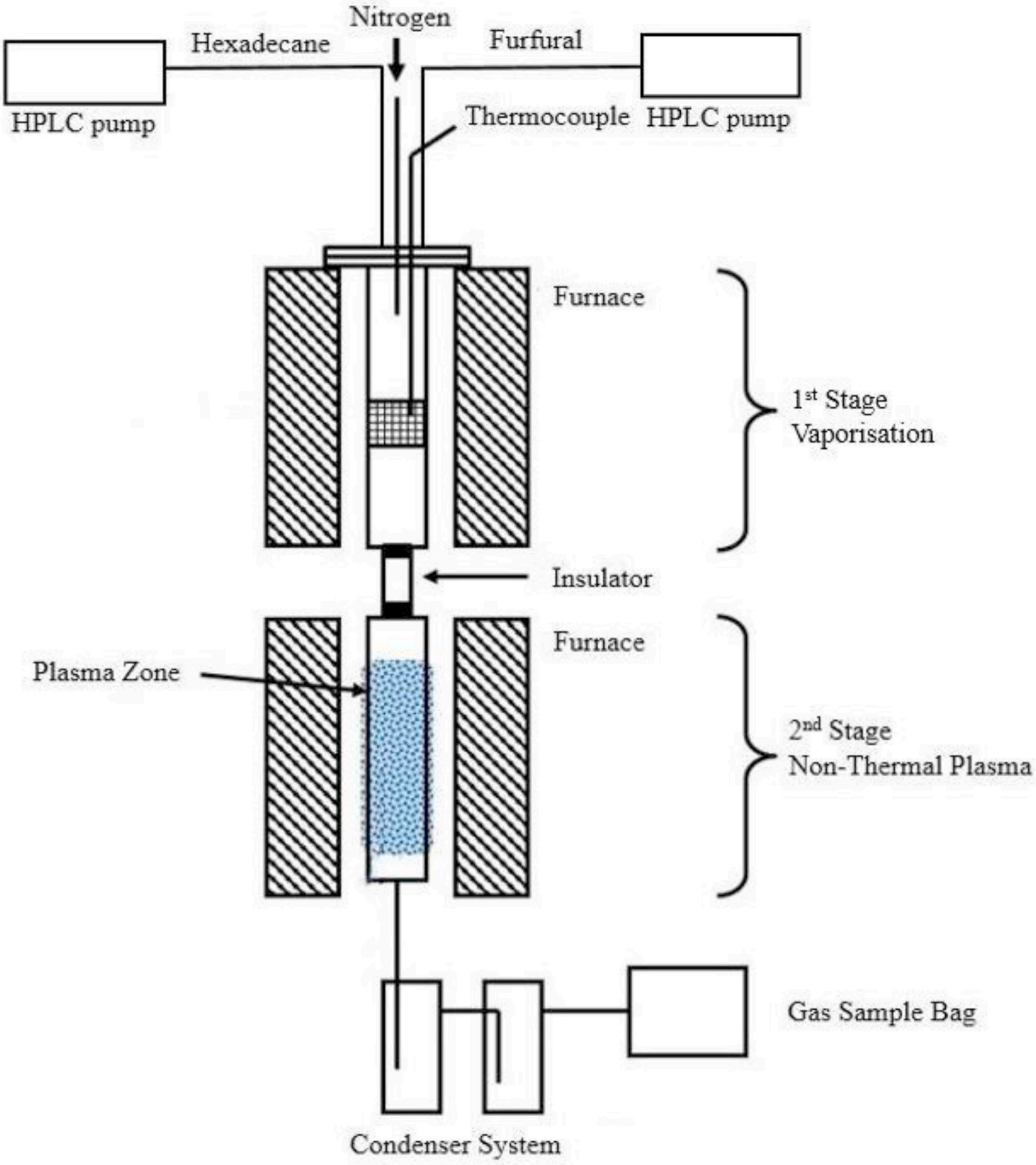

Fig. 1. Schematic diagram of the vaporisation-DBD plasma reactor system.

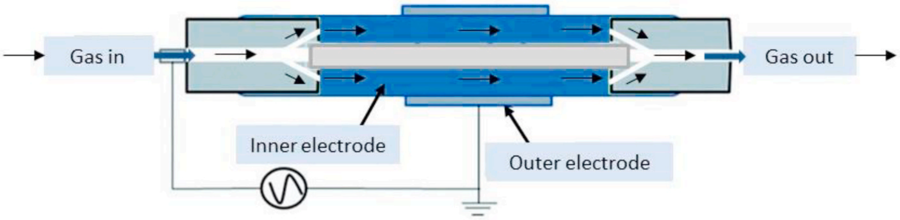

Fig. 2. Schematic diagram of the non-thermal plasma reactor.

Gas and oil yields as well as feedstock conversion were determined utilizing Equation (1), Equation (2) and Equation (3). The mass of gas compounds was computed employing the Ideal Gas Law.

$$Gas\ yield\ (\%) = \frac{mass\ of\ gas}{mass\ of\ injected\ feedstock} \times 100 \tag{1}$$

$$Oil\ yield\ (\ wt.\%) = \frac{Total\ oil\ mass - unreacted\ feedstock\ mass}{Total\ oil\ mass} \times 100 \tag{2}$$

$$Feedstock\ conversion\ (\%) = \left(\frac{injected\ feedstock\ mass - unreacted\ feedstock\ mass}{injected\ feedstock\ mass}\right) \times 100 \tag{3}$$

2.3. Gas analysis

The analysis of the produced gases was conducted using packed column gas chromatography (GC) with a set of Varian 3380C gas chromatographs to determine their composition. For specifying the composition of permanent gases such as H_2, O_2, CO, and N_2, gas chromatography with thermal conductivity detection (GC-TCD) was employed. Argon served as the carrier gas, and a 60–80 mesh molecular sieve column was utilized. Additionally, GC-TCD was utilized to analyze the product gas for CO_2, also with argon as the carrier gas, but employing a HayeSep 60–80 mesh molecular sieve as the column packing material. For the determination of C_1 – C_4 hydrocarbons, gas chromatography with flame ionization detection (GC-FID) was employed. Nitrogen was utilized as the carrier gas, and the column was packed with 80–100 mesh HayeSep packing material.

2.4. Oil analysis

The composition of the product oil collected in the condensers was analyzed using gas chromatography–mass spectrometry (GC–MS), employing a Hewlett-Packard 5280 GC coupled with an HP 5271 ion trap mass spectrometric detector. The GC column utilized was a Restek RTX-5MS fused silica column, measuring 30 m in length and 0.25 mm in internal diameter. The solid phase of the column comprised 95 % dimethyl polysiloxane and 5 % diphenyl, with a film thickness of 25 μm. Helium served as the carrier gas for the GC–MS analysis. Prior to injection into the GC–MS system, the oils were dissolved in dichloromethane. Total ion chromatographic peaks obtained from the GC–MS analysis, along with their respective retention times, were utilized for the identification and quantification of compounds present in the oil. The identification process was supported by referencing the NIST 2008 spectral library, with compounds identified based on an ion mass spectral similarity index exceeding 70 %. Quantification of compounds were calculated using Equation (4) and Equation (5).

$$Concentration\ of\ compound\ x = \frac{peak\ area\ of\ compound\ x}{peak\ area\ of\ standard} \times concentration\ of\ standard \tag{4}$$

$$Mass\ of\ compound\ x = \frac{concentration\ of\ compound\ x}{total\ concentration} \times mass\ of\ produced\ oil \tag{5}$$

2.5. Synergy

The synergistic effect of the interaction between the furfural and hexadecane model compounds can be assessed by comparing the yields of co-pyrolysis products to the calculated theoretical value derived from the sum of yields of the individual components, as demonstrated in Equation (6) [27].

$$y = \sum_{i=1} x_i . y_i \tag{6}$$

In this equation, "y" represents the theoretical value, "yi" stands for the experimental yield, physical properties value, and element content of oils obtained from separate feedstocks, and "x_i" denotes the mass proportion of the feeds in the mixture. A synergistic effect arises when the experimental value is different from the theoretical value.

3. Results and discussion

In this study, the effect of input plasma power on the conversion of furfural, hexadecane and their mixture in relation to the detailed composition of the product oil and gases were investigated. Moreover, the effect of synergistic interaction of the furfural and hexadecane at different input plasma powers was studied. The aim was to understand the influence of hexadecane as a model plastics pyrolysis hydrocarbon model compound acting as a hydrogen donor on the deoxygenation of the bio-oil model oxygenated compound, furfural under non-thermal plasma reaction conditions.

3.1. Product yield from the non-thermal plasma process

Table 1 shows the gas and oil yield, and feed conversion from the vaporisation-non-thermal-plasma processing of furfural, hexadecane, and the furfural: hexadecane mixture at the input powers of 0, 30, 50, and 70 W. At 0 W input plasma power (i.e. no plasma), gaseous products were not produced from furfural, hexadecane, or the mixture. Increasing the input plasma power from 0 to 30 W caused a large increase in the gas yield from furfural (10.65 wt%), and a modest rise in the gas yield from hexadecane (1.03 wt%). A 7.75 wt% increase in the gas yield for the processing of the furfural: hexadecane mixture was observed by changing the input power from 0 W to 30 W. Further increase in the power from 30 to 50 W, and then to 70 W, showed increases in gaseous product yield. In the reactor system, the first stage vaporisation produced volatile furfural and/or hexadecane which pass to the non-thermal plasma reactor where the feedstock molecules collide with energetic species and undergo decomposition by breaking chemical bonds, resulting in the production of ions, atoms, and free radicals. These free radicals can subsequently recombine, generating oil and gas products. Khatibi et al. [27] carried out pyrolysis-non-thermal DBD plasma processing of biomass, polystyrene, and their mixture. They reported that increasing the input power from 0 W to 70 W led to higher gas yields for all feedstocks. The rise in input power resulted in the formation of more gas, affirming the cracking of the pyrolysis vapours into gases within the non-thermal plasma. Nguyen et al. [29], investigated the decomposition of high-density polyethylene into hydrogen and light hydrocarbons using non-thermal plasma. They observed that the total gas yield increased as the input plasma power was increased from 10 W to 60 W. The increase in plasma power resulted in a consistent enhancement in the formation rate of gaseous products. This correlation can be attributed to the greater presence of plasma-active species, thereby accelerating the reaction kinetics.

In the absence of plasma, a very small quantity of oil product, was produced from furfural (0.33 wt%), hexadecane (1.19 wt%), and the mixture (0.19 wt%), representing the amount of the liquid feedstock that reacted in the plasma environment to produce oil (unreacted feedstock was calculated based on Equation (3)). However, when the plasma input power was raised to 30 W, the oil yield showed an increase of around 3, 8, and 14 times for furfural, hexadecane, and the mixture, respectively. The increasing trend for oil yield continued as the input power was raised from 30 W to 50 W and from 50 W to 70 W, resulting in 2.18 wt% oil product produced from non-thermal-plasma processing of furfural. At the same condition, 15.42 wt% oil was produced from hexadecane. The highest oil yield (11.32 wt%) for the mixture was obtained at 70 W.

Raising the input plasma power from 0 W to 70 W significantly enhanced the feed conversion for furfural, hexadecane and the mixture, reaching 19.70 wt% for furfural, 17.30 wt% for hexadecane and 20.46

Table 1
Product yield and feed conversion from the non-thermal plasma processing of furfural, hexadecane and furfural: hexadecane mixture in relation to input plasma power.

Feedstock	Input power (W)	Gas (wt.%)	Total liquid[a] (wt.%)	Product oil in the liquid (wt.%)	Feed conversion to oil and gas (%)
Furfural	0	0	100	0.33	0.33
	30	10.65	89.35	0.97	11.62
	50	13.54	86.46	1.7	15.24
	70	17.91	82.09	2.18	20.09
Hexadecane	0	0	100	1.19	1.19
	30	1.03	98.97	9.34	10.37
	50	1.58	98.42	13.51	15.09
	70	2.23	97.77	15.42	17.65
Furfural-Hexadecane	0	0	100	0.19	0.19
	30	7.75	92.25	2.64	10.39
	50	9.39	90.61	6.50	15.89
	70	10.30	89.70	11.32	21.62

[a] Total liquid consists of unreacted feedstock and product oil.

wt% for the mixture of furfural and hexadecane. Raising the input power can lead to an increase in electron density and gas temperature. Consequently, a higher conversion rate is expected to be attained due to the greater abundance of energetic electrons [30].

3.2. Gas composition from the non-thermal plasma process

Fig. 3(a) illustrates the gas composition yield from non-thermal-plasma upgrading of furfural at 0, 30, 50, and 70 W input plasma powers. No product gas was produced in the absence of the non-thermal plasma. In the presence of plasma, CO is the main gas product compared to other gaseous products at all input powers. In addition, there is a direct relation between increasing power and increasing CO yield (2.91 mmol g^{-1} at 30 W to 5.15 mmol g^{-1} at 70 W). Production of CO which contains oxygen at these high levels shows deoxygenation of furfural has been carried out during the non-thermal-plasma process and that raising the input plasma power increased CO production. CO_2 as another oxygen containing compound was produced in the non-thermal-plasma processing of furfural and its yield was doubled from 0.16 mmol g^{-1} at 30 W to 0.32 mmol g^{-1} at 70 W input power. Hydrogen was also produced during the plasma processing of furfural, plasma power effected its production and raised the yield to 0.23 mmol g^{-1} at 70 W. Methane, ethene, ethane, and propene yields increased with rising input power from 30 to 70 W, whereas, propane and butene and butadiene were produced at almost the same quantities at all input powers.

The composition of the gas products and their yield produced during non-thermal-plasma processing of hexadecane are shown in Fig. 3(b). No gaseous product formation was observed in the absence of the non-thermal plasma. But, for the non-thermal-plasma processing of hexadecane, hydrogen and alkane and alkene gases were the gas products produced. The yields of all gas components produced from hexadecane under non-thermal plasma conditions were enhanced with increasing input power. The majority of the produced gas was hydrogen with a yield of 0.72 mmol g^{-1} at 30 W, rising to 1.17 mmol g^{-1} at 70 W. Methane, butene and butadiene production were doubled when the input power was raised from 30 W to 70 W. In non-thermal plasma reactors involving hydrocarbons, the first stage of the process involves the creation of energetic electrons, typically with a mean energy of 5 eV in DBD reactors [25]. Some of these electrons, possessing adequate energy levels, interact with hydrocarbon molecules, causing the rupture of C–C and C–H bonds, which typically require around 3 eV of energy. These electron-hydrocarbon collisions result in the formation of small activated ions and radicals, which may subsequently recombine to produce hydrogen and lighter hydrocarbons like alkanes and olefins [25].

Fig. 3(c) presents the gas composition and yields from the non-thermal-plasma processing of the mixture of furfural and hexadecane. The yield of gaseous compounds in the absence of plasma upgrading was zero. The main gas compound produced in this process at all powers was CO with a highest yield of 2.56 mmol g^{-1} at the plasma input power of 70 W. CO_2 production was also enhanced with increasing input plasma power. CO and CO_2 production showed that deoxygenation of the mixed feedstock occurred and deoxygenation is dependent on input power, where higher input plasma powers led to higher deoxygenation. Hydrogen was the second major compound at all input powers and its yield continued to rise as the input power was increased. Similarly, all alkanes and alkenes yields were increased when more plasma power was applied.

3.3. Product oil composition from the non-thermal plasma process

Table 2 shows the composition and yield of the oil product produced from the non-thermal plasma processing of furfural as well as the unreacted furfural. Without plasma, only 3.25 mg g^{-1} of feedstock furfural was decomposed, compared with 197.01 mg g^{-1} of furfural was reacted at the input power of 70 W. This indicates that as the input power was increased, there was a higher abundance of energetic electrons and reactive species within the plasma zone. Consequently, collisions become more frequent, leading to an increased probability of electron-driven dissociation reactions and more feedstock reaction. The produced oil compounds can be classified into three main groups: non-oxygenated compounds, one-oxygen, and two-oxygen containing compounds. Toluene, a single ring aromatic compound which was produced at higher input powers, 50 W and 70 W and there was a direct correlation between rising input plasma power and toluene production. Cyclobutene, 2-propenylidene- is another non-oxygenated compound produced at 30, 50, and 70 W plasma powers. Furan, 2-ethyl-5-methyl, pyrazole-4-carboxaldehyde-1-methyl-, and 2-cyclohexen-1-one are the single oxygenated compounds produced during DBD-plasma processing of furfural. In comparison to the feedstock furfural, these compounds contain higher hydrogen and lower oxygen content. Their production rate increased with raising the input power. The dual oxygenated compound, 2-furanmethanol, 5-methyl-, produced a yield of 1.87 mg g^{-1} in the absence of plasma and its production was reduced by around 7.5 times at the higher input power of 70 W to 0.25 mg g^{-1}. This reduction in the yield of dual-oxygenated compounds with increasing power is favourable in terms of deoxygenation.

In our previous study [27], biomass as an oxygenated feedstock source was used to carry out pyrolysis-non-thermal, DBD plasma reactions at different powers. Pyrolysis of biomass produced hydrocarbon and oxygenated volatile compounds which were then subjected to non-thermal plasma processing. It was concluded that the yield of oxygenated compounds in the produced bio-oil decreased as the plasma input power was raised. The yield of ketones, furans, and phenols declined when the input plasma power was increased, indicating that the deoxygenation process took place upon the application of the non-thermal plasma. These findings align with the research conducted by Taghvaei et al. [13], which demonstrated that increasing the applied voltage resulted in a higher degree of deoxygenation concerning

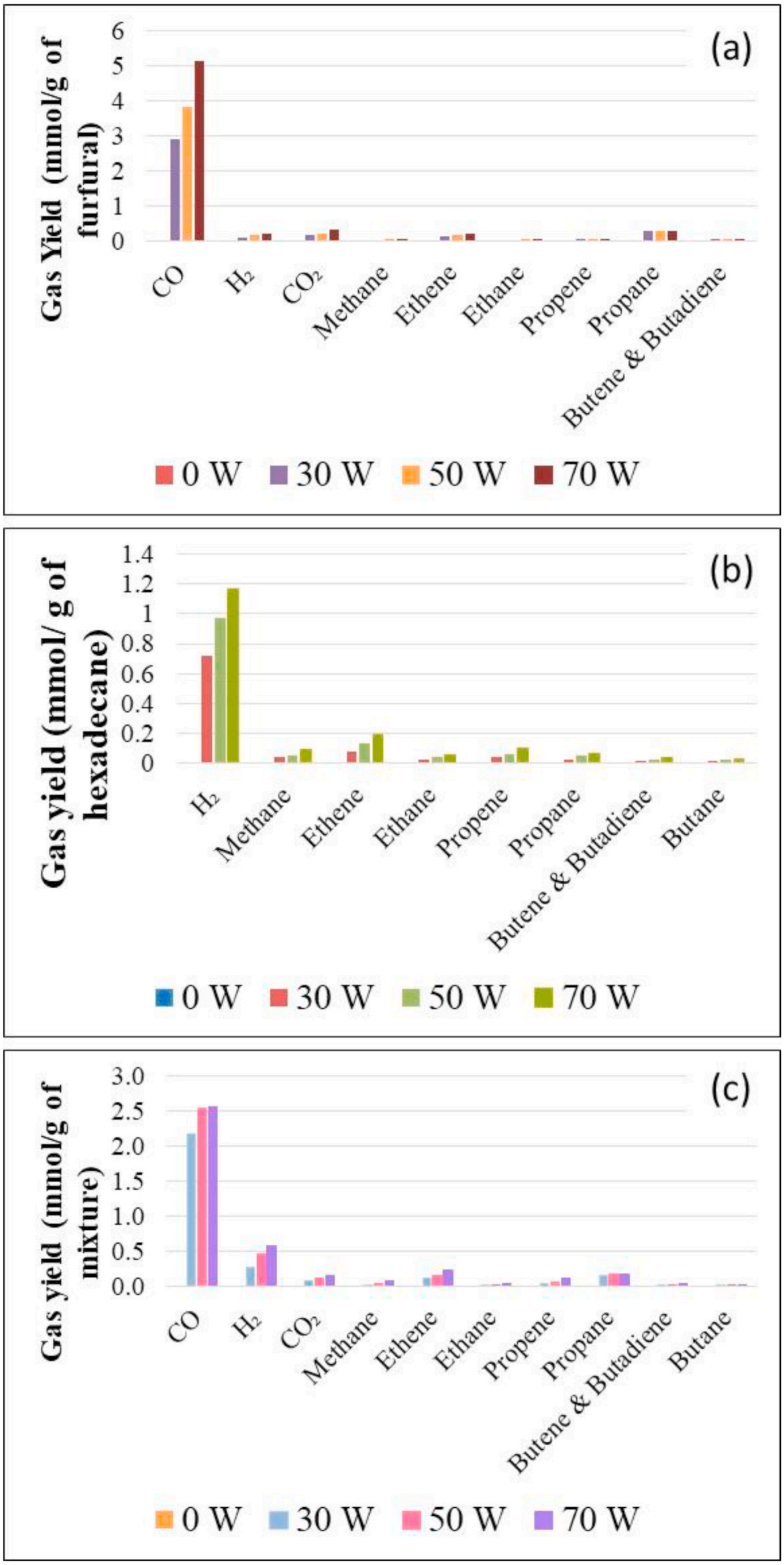

Fig. 3. Gas composition from the non-thermal plasma processing of (a) furfural, (b) hexadecane and (c) a mixture of furfural and hexadecane, in relation to input plasma power.

Table 2
Yield of furfural-derived oil compounds (mg/g of feedstock) from non-thermal-plasma at 0, 30, 50, and 70 W plasma power.

RT (min)	Compound	MW	Formula	0 W	30 W	50 W	70 W
4.672	toluene	92	C_7H_8	0	0	0.06	0.09
5.339	cyclobutene, 2-propenylidene-	92	C_7H_9	0	2.69	2.71	2.29
7.269	furfural	96	$C_5H_4O_2$	996.75	884.84	849.94	802.99
7.768	2-furanmethanol, 5-methyl-	112	$C_6H_8O_2$	1.87	0.73	0.26	0.25
11.163	furan, 2-ethyl-5-methyl	110	$C_7H_{10}O$	0	0	1.33	1.75
14.508	Pyrazole-4-carboxaldehyde-1-methyl-	110	$C_5H_6N_2O$	1.38	3.00	3.42	3.74
14.812	2-cyclohexen-1-one	96	C_6H_8O	0	2.26	6.90	9.79

guaiacol through DBD plasma upgrading. Their study involved hydrodeoxygenation reactions utilizing a quartz glass DBD tubular reactor with argon as the carrier gas for enhancing guaiacol, a representative model compound of lignin pyrolysis oil. By applying a discharge plasma power of 100 W, hydrogen was produced *in-situ*, leading to the breakdown of methyl and methoxyl radicals derived from the lignin pyrolytic oil. The decomposition yielded mono-oxygenated compounds, specifically phenol, methylphenols (2-methylphenol and 4-methylphenol), and dimethylphenols (2,4–2,6 and 3,4-dimethylphenol), alongside benzene, toluene, and xylene. Additionally, trace amounts of anisole, catechol, methylanisoles, cyclohexanol, and trimethylphenols were also identified by Taghvaei et al. [13]. In later work, Taghvaei et al. [31], mentioned that as the applied voltage was increased, there was an upward trend in the selectivity for phenol, benzene, toluene, xylene, while other products such as oxygenated methylphenols and dimethylphenols exhibited a downward trend. These trends were attributed to the enhanced direct demethoxylation of guaiacol due to the stronger electrical field between the two electrodes in the discharge zone resulting from higher voltages. Additionally, methyl radicals can be produced from demethylation and the breaking of the O–CH_3 bond. With an increase in the number of electrons and reactive species, along with higher average electron energy due to increased applied voltage, there was a greater likelihood of decomposition of these methyl radicals (which possess higher bond dissociation energy) into CH_2, CH, and H radicals. This increased decomposition diminished the transalkylation reaction, leading to a reduction in methyl-substituted ring products such as methylphenols and dimethylphenols. Liu et al. [32], investigated steam reforming of toluene as a biomass tar model compound in a DBD plasma reactor. They found that in the plasma reaction without a catalyst, 11 types of organic by-products were identified, including major compounds like benzene, phenol, and (butoxymethyl)-benzene. Additionally, aliphatic compounds such as methyl ester, diol, octadecadienoic acid, and linear compounds like 5,7-dodecadiyn-1,12-diol were detected. These compounds could arise from the cleavage of the toluene

Table 3
Yield of hexadecane-derived oil compounds (mg g^{-1} of feedstock) from non-thermal-plasma at 0, 30, 50, and 70 W plasma power.

RT (min)	Compound	MW	Formula	0 W	30 W	50 W	70 W
3.087	Heptene	98	C_7H_{14}	0	0.16	0.26	0.41
3.211	Heptane	100	C_7H_{16}	0	0.23	0.37	0.47
4.939	Heptane, 3-methyl-	114	C_8H_{18}	0	0	0	0.26
5.565	Octene	112	C_8H_{16}	0	0.39	0.45	1.01
5.897	Octane	114	C_8H_{18}	0	0.59	0.83	1.29
8.816	Octane, 4-methyl-	128	C_9H_{20}	0	0	0	0.34
10.398	Nonene	126	C_9H_{18}	0	0.53	0.75	1.96
10.921	Nonane	128	C_9H_{20}	0	0.70	0.96	1.76
14.334	Nonane, 3-methyl	142	$C_{10}H_{22}$	0	0	0	0.27
16.948	Decene	140	$C_{10}H_{20}$	0	0.91	0.93	2.53
17.578	Decane	142	$C_{10}H_{22}$	0	1.00	1.28	2.38
21.445	Decane, 3-methyl	156	$C_{11}H_{24}$	0	0	0	0.28
23.365	Undecene	154	$C_{11}H_{22}$	0	0.64	1.19	3.42
23.799	Undecane	156	$C_{11}H_{24}$	0	1.01	1.39	2.56
26.810	Undecane, 5-methyl	170	$C_{12}H_{26}$	0	0	0	0.27
27.606	Dodecene	168	$C_{12}H_{24}$	0	0.75	1.09	2.86
27.920	Dodecane	170	$C_{12}H_{26}$	0	0.91	1.31	2.40
30.829	Tridecene	182	$C_{13}H_{26}$	0	0.70	1.00	3.18
31.209	Tridecane	184	$C_{13}H_{28}$	0.45	0.98	1.42	2.53
33.884	Tetradecene	196	$C_{14}H_{28}$	0.27	0.67	1.13	2.51
34.113	Tetradecane	198	$C_{14}H_{30}$	0	1.15	1.68	2.26
36.588	Pentadecene	210	$C_{15}H_{30}$	0	0.26	0.36	0.65
36.794	Pentadecane	212	$C_{15}H_{32}$	1.75	1.91	1.98	2.20
38.256	Hexadecene	224	$C_{16}H_{32}$	1.68	48.71	61.56	53.53
39.476	Hexadecane	226	$C_{16}H_{34}$	988.13	897.26	851.29	827.00
40.446	Heptadecyne	236	$C_{17}H_{32}$	5.79	0	0	0
40.556	Heptadecene	238	$C_{17}H_{34}$	0	8.79	12.17	11.45
41.684	Heptadecane	240	$C_{17}H_{36}$	0.85	1.27	1.33	1.23
42.665	Octadecene	252	$C_{18}H_{36}$	0	8.92	14.37	14.16
43.925	Octadecane	254	$C_{18}H_{38}$	1.08	1.91	2.43	2.42
44.285	Nonadecene	266	$C_{19}H_{38}$	0	5.11	10.59	11.30
46.176	Nonadecane	268	$C_{19}H_{40}$	0	0.46	0.69	0.79
47.099	Eicosene	280	$C_{20}H_{40}$	0	2.87	5.69	6.93
48.381	Eicosane	282	$C_{20}H_{42}$	0	0.26	0.40	0.52
49.554	Heneicosene	296	$C_{21}H_{42}$	0	0.61	3.50	5.06
50.412	Heneicosane	296	$C_{21}H_{44}$	0	0	0.68	1.05
51.984	Docosene	308	$C_{22}H_{44}$	0	0	1.12	2.59
52.114	Docosane	310	$C_{22}H_{46}$	0	0	0	0.39
52.807	Tricosene	322	$C_{23}H_{46}$	0	0	0	1.50

ring and the subsequent recombination and hydrogenation of the resulting intermediate fragments.

Table 3 shows the oil composition and their yield produced during non-thermal-plasma processing of hexadecane at 0, 30, 50, and 70 W input plasma powers. This table also contains the yield of unreacted hexadecane and indicates that only 11.87 mg g^{-1} of it was decomposed in the absence of plasma. However, in the presence of the non-thermal plasma, hexadecane conversion was markedly increased, reaching 173 mg g^{-1} for the reaction at 70 W. The oil products from hexadecane cracking are categorized into alkane, alkene, and methyl alkane groups (the compounds with carbon number in the range of C_8 – C_{12}). The compounds appeared in a specific order regarding retention time of alkene, alkane, and finally methyl alkane with the alkane as the largest concentration compound. Without applying plasma, limited cracking was observed for C_{13}–C_{18} hydrocarbons. Elevating power to 30 W and 50 W generated alkenes and alkanes from C_7–C_{22} hydrocarbons, and by raising the input power to 70 W, methyl alkanes started to be produced. Moreover, the yield of alkanes and alkenes was also enhanced at 70 W compared to 50 W except for a few heavy hydrocarbons, including hexadecene, heptadecene, heptadecane, octadecene, and octadecane. The yield of light products (lighter than hexadecane) were calculated based on the division of the sum of the yields of light hydrocarbons to the total yield of all oil yield (light and heavy hydrocarbons). Only 35 % of the oil products were light hydrocarbons in the absence of plasma, while this amount increased to 60.6 % at the input power of 70 W, that is, the cracking increased by 25.6 % by raising input plasma power from 30 W to 70 W. Khani et al. [33], working on hexadecane cracking in a DBD non-thermal plasma reactor reported that collisions between high-energy electrons and n-hexadecane molecules resulted in the production of various hydrocarbons; lighter hydrocarbons such as C_6 to C_{15}, in addition to some heavier hydrocarbons formed from the recombination of activated radicals. Both saturated and unsaturated products were observed in their results.

The oil compounds and their yields produced from the mixture of furfural and hexadecane via the non-thermal-plasma process at the input plasma powers of 0, 30, 50, and 70 W are displayed in Table 4. Unreacted furfural and hexadecane are also shown in Table 4. As the power was gradually raised from 0 W to 70 W, the amount of unreacted furfural decreased from 521.02 mg g^{-1} to 409.72 mg g^{-1}, which is a 21.4 % decrease and the amount of unreacted hexadecane declined by 19.2 % from 477.08 mg g^{-1} to 385.71 mg g^{-1}, suggesting significant interaction of the furfural and hexadecane. Toluene and cyclobutene, 2-propenylidene- are the two non-oxygenated compounds produced from furfural. The yield of toluene increased with increasing input power from 0 mg g^{-1} at 0 W to 0.53 mg g^{-1} at 70 W. The dual-oxygenated compound which was produced in the non-thermal plasma processing of pure furfural, was not produced in the mixture, suggesting the deoxygenation of compounds with high oxygen number. Table 4 shows that the three mono oxygenated compounds $C_7H_{10}O$, $C_5H_6N_2O$, C_6H_8O) showed enhanced yields when the input power was applied, rising from 0.82 mg g^{-1} in the absence of plasma to 38.4 mg g^{-1} at 70 W power. The other compounds produced were alkanes and alkenes. In the absence of plasma, there were only small quantities of a few hydrocarbons, including tridecane, tetradecene, and pentadecane. However, at the input power of 30 W, more hydrocarbons were produced compared to 0 W. By raising the power to 50 W and then 70 W, C_8–C_{18} alkanes and alkenes were produced and there was direct correlation between power and the yield of the hydrocarbons except for some heavy hydrocarbons (tetradecane, hexadecene, heptadecene, octadecene). Moreover, mixing furfural and hexadecane eliminated some of heaviest hydrocarbons in the range from C_{19}–C_{23}.

3.4. Synergistic interaction of furfural and hexadecane

Fig. 4 indicates the synergistic effect in relation to product yields and feed conversion from the non-thermal-plasma processing of the mixture of furfural and hexadecane. Without plasma, the synergy related to gas yield was zero because gas was not produced using furfural, hexadecane, or their mixture. Oil yield and feed conversion synergies were negative when there was no plasma was applied. However, applying the plasma to the process with the power of 30 W generated a positive synergy of 1.91 % for the gas yield, while oil yield and feed conversion were still negative. When the plasma input power was raised to 50 W, gas yield synergy remained in the same level and oil yield was less negative

Table 4
Yield of a furfural: hexadecane mixture-derived oil compounds (mg g^{-1} of feedstock) from non-thermal-plasma at 0, 30, 50, and 70 W plasma power.

RT (min)	Compound	MW	Formula	0 W	30 W	50 W	70 W
4.705	Toluene	92	C_7H_8	0	0	0.09	0.53
5.365	cyclobutene, 2-propenylidene-	92	C_7H_9	0	0.58	1.60	0.85
5.516	Octene	112	C_8H_{16}	0	0	0.49	2.97
5.837	Octane	114	C_8H_{18}	0	0	2.09	2.32
7.299	Furfural	96	$C_5H_4O_2$	521.02	506.15	472.20	409.72
10.321	Nonene	126	C_9H_{18}	0	0	2.21	5.31
10.840	Nonane	128	C_9H_{20}	0	0	0.66	1.15
11.207	Furan, 2-ethyl-5-methyl	110	$C_7H_{10}O$	0	1.12	2.63	5.97
14.509	Pyrazole-4-carboxaldehyde-1-methyl-	110	$C_5H_6N_2O$	0.82	2.67	3.12	7.68
14.775	2-Cyclohexen-1-one	96	C_6H_8O	0	6.69	6.67	24.75
16.851	Decene	140	$C_{10}H_{20}$	0	0.50	2.61	6.77
17.486	Decane	142	$C_{10}H_{22}$	0	0.28	0.78	2.44
23.334	Undecene	154	$C_{11}H_{22}$	0	0.67	3.65	8.50
23.785	Undecane	156	$C_{11}H_{24}$	0	0.45	2.03	1.60
27.726	Dodecene	168	$C_{12}H_{24}$	0	0.68	3.38	5.95
28.054	Dodecane	170	$C_{12}H_{26}$	0	0.41	1.25	1.31
31.205	Tridecene	182	$C_{13}H_{26}$	0	0.61	1.92	4.39
31.474	Tridecane	184	$C_{13}H_{28}$	0.18	0.48	0.96	1.65
34.227	Tetradecene	196	$C_{14}H_{28}$	0.07	0.67	1.29	3.56
34.462	Tetradecane	198	$C_{14}H_{30}$	0	0.36	0.77	0.71
36.973	Pentadecene	210	$C_{15}H_{30}$	0	0.10	0.23	0.49
37.181	Pentadecane	212	$C_{15}H_{32}$	0.83	0.62	0.80	0.94
38.799	Hexadecene	224	$C_{16}H_{32}$	0	7.49	17.23	9.36
39.789	Hexadecane	226	$C_{16}H_{34}$	477.08	392.01	374.97	385.71
40.098	Heptadecene	238	$C_{17}H_{34}$	0	0	0.99	0.67
42.098	Heptadecane	240	$C_{17}H_{36}$	0	0	0	0.77
44.180	Octadecene	252	$C_{18}H_{36}$	0	0	0.73	0
44.352	Octadecane	254	$C_{18}H_{38}$	0	0	0.74	0.94

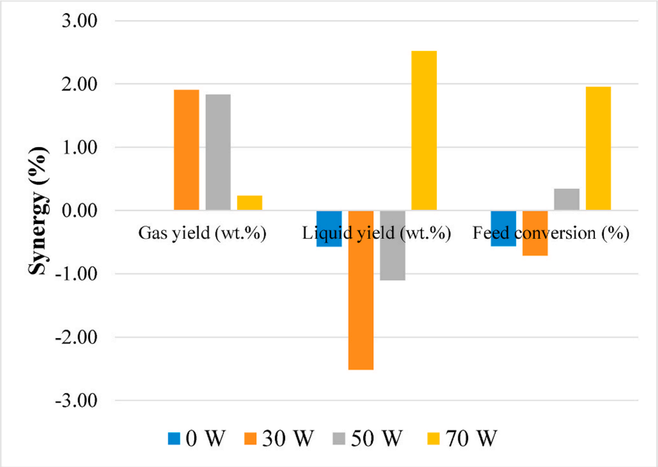

Fig. 4. Synergistic effect on product yield for non-thermal plasma processing of the furfural: hexadecane mixture at 0, 30, 50, and 70 W plasma power.

compared to oil synergy in 30 W. Raising the power to 70 W generated a higher positive synergy in gas yield, oil yield, and feed conversion at 0.23 %, 2.52 % and 1.96 %, respectively.

Chen et al. [34], investigated the synergistic effect in the co-pyrolysis of biomass in the form of waste newspaper with high-density polyethylene. They reported that the co-pyrolysis resulted in a noticeable decrease in gas yield, while the yield of the oil phase was significantly enhanced. This indicated a synergistic effect from co-pyrolysis, resulting in higher oil yield and lower gas yield. These results were attributed to the transfer reaction of hydrogen atoms and the generation of free radicals during the pyrolysis of HDPE. These reactions promote cross-reactions between waste newspaper and HDPE during co-pyrolysis. This effect interfered with the degradation of functional groups bonded in the cellulose structure of waste newspaper, inhibiting the release of gaseous products with low molecular weight and favouring the formation of organic compounds with high molecular weight in the oil phase.

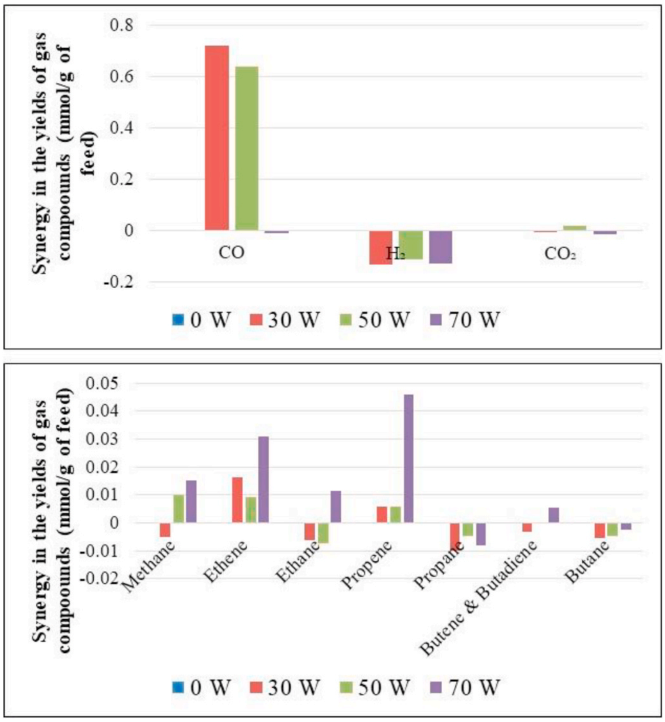

Fig. 5. Synergistic effect on gas components yield (mmol/g of feedstock) for non-thermal plasma processing of the furfural: hexadecane mixture at 0, 30, 50, and 70 W plasma power.

Fig. 5 indicates the synergistic effect in relation to the yield of individual gas components from the non-thermal-plasma processing of the mixture of furfural and hexadecane at different input plasma powers. At the input power of 30 W, the synergy for all the gas compounds are negative except for carbon monoxide, ethene, and propene. When the power was increased to 50 W, the yield of CO, CO_2, methane, ethene, propene, butene and butadiene from non-thermal-plasma processing of the mixture were higher than the gas yields from plasma processing of furfural and hexadecane alone. The negative synergy for hydrogen may indicate that hydrogen is being consumed in the hydrodeoxygenation process and results in the production of carbon oxides, mainly CO. The gas yield synergies for CO, CO_2, and H_2 were negative when the plasma power was increased to 70 W, however, the production of most alkane and alkene gases showed the highest synergistic effect compared to lower input powers, (except for propane and butane). Increasing the plasma power from 0 W to 70 W resulted in higher yields of gases. This increase in input plasma power led to elevated electric fields and electron temperatures, generating more energetic electrons, radicals, and other reactive species. Consequently, there was an increase in the breakdown of volatile molecules, resulting in higher gas yields [27].

Yuan et al. [35], investigated synergistic effects during the co-pyrolysis of cellulose and high-density polyethylene. They concluded that the interaction between cellulose and high-density polyethylene facilitated the generation of oxygen containing molecules, such as H_2O, CO/C_2H_4, and CO_2, with this effect becoming more pronounced as the percentage of HDPE was increased. This effect could be attributed to the promotion of decomposition of cellulose pyrolytic products by the presence of the polyethylene, resulting in the release of a large number of small-molecule volatiles. The promotion effect primarily occurred during the decomposition of cellulose, indicating that the release of gas products from cellulose could be facilitated by the presence of polyethylene during the co-pyrolysis process.

Table 5 demonstrates the effect of synergy on oil compound yields produced in the non-thermal plasma processing of furfural and hexadecane at 0, 30, 50, and 70 W input plasma power. Toluene is the single ring aromatic compound produced at higher input powers of 50 W and 70 W, the data shows that raising the power intensified toluene production from the processing of the mixture with a positive synergy of 0.49 at 70 W. The formation of 2-furanmethanol, 5-methyl- with dual-oxygen in its structure was supressed in the mixture at all input powers, whereas, the synergistic effect is positive for compounds containing one oxygen. Huang et al. [36], carried out catalytic fast pyrolysis of biomass and low-density polyethylene over hierarchical HZSM-5 to investigate the synergistic reaction mechanism. They found that the transfer of hydrogen free radicals from the polyethylene derived hydrocarbons to the biomass-derived oxygenates facilitated the deoxygenation reaction of oxygenates. The suggested that the Diels-Alder reaction was the key synergistic reaction between furans and olefins, significantly enhancing the yield of hydrocarbon aromatic compounds.

The hydrocarbons shown in Table 5 were classified into two main groups: light and heavy hydrocarbons. In the case of the light hydrocarbons, increasing the plasma power to 30 W generated more compounds with positive synergy compared to 0 W. Raising the power to 50 W and 70 W in relation to the light hydrocarbons caused positive synergy for most of the light hydrocarbon oil products and it was also observed that increasing power intensified the amount of positive synergy. In general, the synergy for light hydrocarbons at 0 W and 30 W are small negative amounts while increasing the power to 50 W and 70 W enhanced the synergy to 15.91 % and 31.14 %, respectively. This suggests that mixing the furfural and hexadecane at higher input powers was desirable as the production of light hydrocarbons was increased compared to plasma processing of the pure furfural and hexadecane feedstock.

Table 5

Synergy in the yields of oil compounds derived from furfural and hexadecane (mg g^{-1} of feedstock) at 0, 30, 50, and 70 W plasma power.

Compound	Synergy (%)			
	Input Plasma power (W)			
	0 W	30 W	50 W	70 W
toluene	0.00	0.00	0.06	0.49
cyclobutene, 2-propenylidene-	0.00	−0.76	0.25	−0.29
2-Furanmethanol, 5-methyl-	−0.93	−0.36	−0.13	−0.13
Furan, 2-ethyl-5-methyl	0.00	1.12	1.97	5.09
Pyrazole-4-carboxaldehyde,1-methyl-	0.13	1.17	1.41	5.81
2-Cyclohexen-1-one	0.00	5.57	3.22	19.86
Light Hydrocarbons				
Heptene	0.00	−0.08	−0.13	−0.21
Heptane	0.00	−0.11	−0.19	−0.23
Heptane, 3-methyl-	0.00	0.00	0.00	−0.13
Octene	0.00	−0.19	0.27	2.46
Octane	0.00	−0.30	1.67	1.67
Octane, 4-methyl-	0.00	0.00	0.00	−0.17
Nonene	0.00	−0.27	1.83	4.33
Nonane	0.00	−0.35	0.18	0.27
Nonane, 3-methyl	0.00	0.00	0.00	−0.14
Decene	0.00	0.05	2.14	5.50
Decane	0.00	−0.22	0.14	1.25
Decane, 3-methyl	0.00	0.00	0.00	−0.14
Undecene	0.00	0.35	3.05	6.79
Undecane	0.00	−0.05	1.33	0.33
Undecane, 5-methyl	0.00	0.00	0.00	−0.14
Dodecene	0.00	0.30	2.84	4.52
Dodecane	0.00	−0.05	0.59	0.11
Tridecene	0.00	0.26	1.42	2.80
Tridecane	−0.04	−0.01	0.25	0.39
Tetradecene	−0.06	0.34	0.73	2.31
Tetradecane	0.00	−0.21	−0.07	−0.43
Pentadecene	0.00	−0.03	0.05	0.16
Pentadecane	−0.05	−0.34	−0.20	−0.17
Total Light Hydrocarbons	**−0.15**	**−0.92**	**15.91**	**31.14**
Heavy Hydrocarbons				
Hexadecene	−0.84	−16.87	−13.55	−17.41
Heptadecyne	−2.89	0.00	0.00	0.00
Heptadecene	0.00	−4.39	−5.10	−5.06
Heptadecane	−0.43	−0.64	−0.66	0.15
Octadecene	0.00	−4.46	−6.45	−7.08
Octadecane	−0.54	−0.95	−0.48	−0.27
Nonadecene	0.00	−2.56	−5.30	−5.65
Nonadecane	0.00	−0.23	−0.35	−0.39
Eicosene	0.00	−1.43	−2.85	−3.46
Eicosane	0.00	−0.13	−0.20	−0.26
Heneicosene	0.00	−0.31	−1.75	−2.53
Heneicosane	0.00	0.00	−0.34	−0.52
Docosene	0.00	0.00	−0.56	−1.29
Docosane	0.00	0.00	0.00	−0.20
Tricosene	0.00	0.00	0.00	−0.75
Total Heavy Hydrocarbons	**−4.70**	**−31.97**	**−37.58**	**−44.73**

In the case of the heavy hydrocarbons, the synergy at 0 W (no plasma) was zero for most of the compounds. By changing the power from 0 W to 30 W, the number and quantity of compounds with negative synergy increased for the heavy hydrocarbons. Increasing the power to 50 W and 70 W generated more compounds with negative amounts in synergy, also the synergies were more negative with increase of the input plasma power. The synergy for the total heavy hydrocarbons was −4.70 % in the absence of plasma. As the power was raised from 0 W to 70 W, the synergy tended to be more negative with −44.73 % at 70 W. This indicates that mixing furfural and hexadecane suppressed the formation of heavy hydrocarbons and increasing the power intensified the decrease in heavy hydrocarbons production and increasing the formation of light hydrocarbons.

3.5. *Oxygen distribution in gas and oil products*

In order to further understand the influence of synergistic interaction between the oxygenated furfural and the hydrocarbon hexadecane, the distribution of oxygenated species in the gas and oil phases was explored. Fig. 6 shows the distribution of oxygen in the gas and oil products produced from the non-thermal plasma processing of furfural and the furfural: hexadecane mixture. Fig. 6(a) and (b) also show the amount of reacted furfural as the oxygen containing feedstock at different input powers. It is evident that the rate of furfural consumption increased by raising the input plasma power reaching, 2.05 mmol g^{-1} furfural and 0.75 mmol g^{-1} in the mixture at 70 W power input, due to the higher energetic electrons at higher powers. Most of the produced oxygen was in the gas phase in the form of CO and CO_2 comprising around 90 % of the total produced oxygen from processing of furfural and the mixture. Increasing the input plasma power enhanced the oxygen yield in the gas products, including CO and CO_2 to 5.15 and 0.32 mmol g^{-1} furfural at 70 W respectively. For the mixture, the oxygen yield of CO and CO_2 at 70 W was 2.56 and 1.43 mmol g^{-1}, respectively. The oxygen proportion in the oil products was small at all plasma powers (Fig. 6(b) and (d), indicating that non-thermal plasma processing of the oxygenated hydrocarbon furfural and the mixture containing furfural produces a product oil low in oxygen. The oxygen yield in the oil compounds containing one oxygen atom tended to increase with increasing plasma power, but the oxygen content for the two-oxygen containing compounds (2-furanmethanol, 5-methyl- ($C_6H_8O_2$)) decreased during the non-thermal plasma processing of furfural with raising the power. Oxygen was not produced in the form of $C_6H_8O_2$ from the mixture because of the synergy between furfural and hexadecane.

3.6. *The synergistic, non-thermal plasma deoxygenation process*

This study suggests that there is minimal interaction of the model bio-oil and plastics pyro-oil model compounds in the absence of the non-thermal plasma environment. However, in the presence of the plasma, there is clearly interaction of the furfural and hexadecane which leads to lower formation of dual-oxygenated compounds and heavy hydrocarbons while favourable to the formation of light hydrocarbons. In addition, formation of single ring aromatic compounds was increased. Raising the input plasma power increased the reactive environment in the plasma and led to the interaction of oxygenated compounds and the hexadecane hydrocarbon, hence, CO and CO_2 production were increased. The negative synergy of H_2 for the mixture at all input powers confirms that hydrogen was consumed in the deoxygenation reactions. This is due to the direct correlation between the increase in the number of energetic electrons and reactive species in the plasma zone and the rising applied voltage. Increasing the applied plasma power generates a stronger electric field, subsequently raising the energy, temperature, and electron density within the discharge area. This, in turn, increases the likelihood of electron-driven dissociation reactions such as ionization, excitation, and gas molecule dissociation. Consequently, there is a rise in the formation of reactive species within the plasma zone, resulting in heightened feedstock conversion [28,31,37–39].

Fan et al. [40], investigated the co pyrolysis with non-thermal-plasma processing of cellulose and polyethylene. They reported that converting cellulose-derived furfural was challenging, but increasing the polyethylene ratio led to more olefin production and facilitated furfural deoxygenation. The presence of hydrogen-containing radicals derived from polyethylene pyrolysis proved beneficial for the deoxygenation of biomass-derived oxygenates. Moreover, deoxygenation was inclined to generate highly reactive oxygen radicals under the influence of the non-thermal plasma. These oxygen radicals, in turn, facilitated the cracking and decomposition of long-chain olefins or olefinic radicals. In our previous work [27], biomass and polystyrene were co-pyrolyzed and the produced volatiles were upgraded in a DBD non-thermal plasma reactor at different input powers. Applying non-thermal plasma to the process led to a significant reduction in the presence of oxygenated compounds in the product oil, nearly reaching zero at input plasma powers of 50W and 70W. Hassan et al. [41], studied

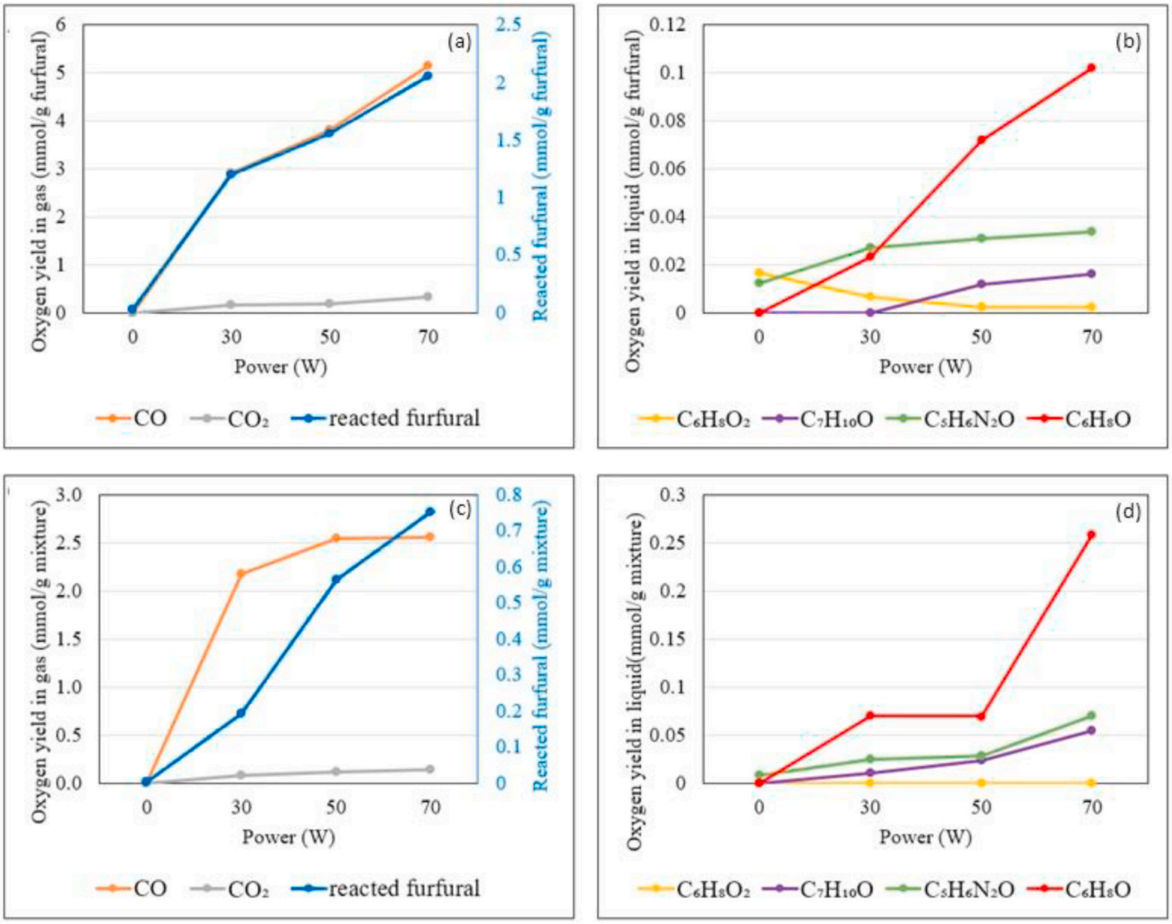

Fig. 6. Oxygen yield (mmol/g injected feedstock) in (a) the product gas and (b) the product oil from the non-thermal plasma processing of furfural and oxygen yield in (c) the product gas and (d) the product oil from the non-thermal plasm processing of the furfural and hexadecane mixture.

co-pyrolysis of biomass in the form of sugarcane bagasse and high-density polyethylene. They reported that the synergistic interaction resulted in a higher oil yield than the theoretical value. The positive synergistic effects on the production of high-value organic compounds such as alcohols, hydrocarbons, and aromatics, along with the inhibition of oxygenated compounds, were most prominent at 600 °C and a 40:60 polyethylene: biomass: ratio. The biomass derived hydroxyl radicals facilitated the secondary cracking of primary volatiles from the polyethylene, promoting the formation of aliphatic compounds with lower carbon numbers.

There are some studies exploring the decomposition of model compounds in a non-thermal plasma reactor and the effect of increasing power on the decomposition. Taghvaei et al. [31], studied hydrodeoxygenation of guaiacol in a DBD plasma-catalytic reactor. They obtained the maximum conversion (54 %) and deoxygenation (51 %) at 12 kV applied voltage and 3 l h^{-1} feed flow rate. They showed that increasing the applied voltage typically improves guaiacol conversion and deoxygenation. Saleem et al. [37], explored the decomposition of benzene as a tar model compound in a gas mixture (CO_2, H_2, CO, and CH_4) using a DBD non-thermal plasma reactor. They demonstrated that the decomposition of benzene was raised proportionally with the increase in the Specific Input Energy (SIE). The decomposition of the benzene increased from 49.9 % to 96 % with the rise in SIE from 2.05 to 16.4 kWh m^{-3}. The SIE is typically regulated through flow rate and input power. In their work, the flow rate remained constant while the SIE significantly increased due to an increase in input power. They also reported that selectivity towards individual C_2–C_5 hydrocarbons was enhanced as the SIE was increased from 2 kWh m^{-3} to 16 kWh m^{-3}. The impact of electrons generates CH_3, CH_2, and CH radicals, which can combine to form lower molecular weight hydrocarbons. Sasujit et al. [38], designed a reverse vortex flow gliding arc plasma for the elimination of tar model compounds, employing naphthalene as a representative model compound. A peak removal efficiency of approximately 85 % was achieved with an input power of 0.13 kWh m^{-3}, resulting in an energy utilization efficiency of about 4.60 g kWh^{-1}, alongside an applied high voltage of 15 kV. It was observed that the efficiency of naphthalene removal increased in tandem with the rise in applied voltage and power. In a later paper, Saleem et al. [28], investigated the decomposition of benzene with CH_4 using a DBD reactor. They found that the decomposition of benzene is observed to rise alongside an increase in input power. They also found that the yield of hydrogen and lower hydrocarbons increased as power was increased due to the abundance of reactive species. Hydrogen radicals were produced through the abstraction of H from benzene and CH_4. These radicals combine to form hydrogen. The total yield of hydrogen depended on the decomposition of tar compounds and methane carrier gas. The decomposition of methane also produced C_2–C_5 hydrocarbons. The impact of energetic electrons generated various radicals such as CH_3, CH_2, CH, and H, which could combine to produce different lower hydrocarbons. The yield of C_2–C_5 hydrocarbons were also enhanced with raising power. Dahiru et al. [39], studied the effect of input power, carrier gases and moisture content on the removal of benzene in dry air and humidified air in a DBD non-thermal plasma reactor. As the plasma power was increased from 2 to 10 W in both dry and humidified air, the benzene removal efficiency escalated from 16.8 % to 56.8 % and from 24.5 % to 77.9 %, respectively. Khani et al. [33], studied the cracking of hexadecane in a DBD non-thermal plasma reactor. They found that increasing the applied voltage and working gas flow rate improved both the conversion and cracking percentages of the hexadecane. The highest conversion percentage achieved was 9.26 % when the applied voltage was 12 kV and the methane flow rate was 50 sccm with a cracking percentage of 84.34 %. Saleem et al. [42], investigated the reactions of toluene in a DBD non-thermal plasma reactor with H_2 as the carrier gas. They found that with the increase in plasma power, the efficiency of toluene decomposition increased, as did the overall selectivity towards lower hydrocarbons. Furthermore, the selectivity of C_1–C_5 hydrocarbons increased with higher power levels, indicating the breakdown of the aromatic ring at elevated plasma power.

Some studies investigated the effect of non-thermal plasma reactions on gas composition yields. Saleem et al. [30], reported on the decomposition of toluene using a DBD non-thermal plasma reactor with CO_2 as the carrier gas. They observed the yield of CO was raised with Specific Input Energy (increasing power from 5 W to 17 W), likely to be due to electron impact dissociation reactions. With higher power, the electron density increases, thereby contributing to an increased yield of CO. The yield of H_2 increased with rising Specific Input Energy, and was attributed to the greater abundance of reactive species at higher supplied power. At lower power levels, reactive species abstracted the H from the methyl group due to its minimum bond dissociation energy in the toluene molecule. At higher powers, the presence of more reactive species and energetic electrons led to an increase in hydrogen yield as a result of aromatic ring cleavage. Khatibi et al. [27], performed pyrolysis-non-thermal-plasma of polystyrene, biomass, and a mixture of biomass and polystyrene in a DBD reactor. For polystyrene, the yields of all gas products increased with the raising of input plasma power. For biomass, the introduction of non-thermal plasma led to higher yields of carbon monoxide, carbon dioxide, hydrogen, and methane. For the mixture, raising plasma power resulted in higher yields of carbon monoxide, carbon dioxide, hydrogen, methane, and C_2–C_4 hydrocarbons in the gas phase. Wang et al. [43], investigated a two-stage pyrolysis with DBD non-thermal plasma process for H_2 production from cellulose. They observed an increase in all gas yields, including CO, CO_2, CH_4, C_2–C_3, and H_2, with the rise in plasma input power from 0 W to 15 W. Nguyen et al. [29], reported that introducing a non-thermal plasma stage alongside the thermal stage outperformed the thermal case, attributed to the presence of vibrationally excited species. Increasing the input power enhanced the production of hydrogen and methane, which became predominant components at higher input powers (40 W–60 W). Under high plasma power conditions, hydrogen emerged as the predominant product, attributed to the endothermic cracking of long-chain C–H fragments, a process promoted by the elevated temperatures observed at high plasma power levels. Blanquet et al. [44], investigated H_2 production from waste biomass through a pyrolysis-non-thermal plasma-catalytic reforming process. They reported that the yields of hydrogen, methane, carbon monoxide, and carbon dioxide increased as the input plasma power was raised from 40 W to 80 W. Xu et al. [45], explored the reforming of pyrolysis volatiles derived from biomass using a combined pyrolysis and plasma-catalysis technology for H_2 production. Their experiments, conducted at various discharge powers in the non-thermal plasma reactor without catalyst and steam, revealed a significant increase in the yields of all gaseous products, particularly H_2 and CO, compared to thermal-only conditions. This enhancement was primarily attributed to the greater abundance of electrons generated through intensified micro-discharges in the catalytic non-thermal plasma process. The increased electron presence offers additional reaction channels and reactive species, thereby facilitating more reaction processes. Meng et al. [46], investigated the gas and tar composition produced from fluidized bed gasification of coal processed through a DBD plasma reactor. They observed that increasing the specific energy density resulted in the formation of more alkanes and fewer aromatics in the gas phase. Within the plasma discharge, aromatic hydrocarbons and other cyclic substances undergo conversion into aliphatic hydrocarbons under the impact of high-energy electrons.

Overall, the process of non-thermal plasma processing of the oxygenated hydrocarbon model compound, furfural, shows that the non-thermal plasma reaction environment converts the furfural into a product oil that has a low oxygenated compound content. Although the oil yield from furfural is quite low at 2.18 wt% at 70 W (Table 1), the oil has a low content of oxygenated compounds (Fig. 6(b)). The deoxygenation is represented by expulsion of the oxygen as CO and CO_2. The role of hexadecane as a model hydrocarbon typically found in the product oil from polyethylene and polypropylene plastic, is to aid cracking reactions and provide a source of hydrogen for hydrodeoxygenation reactions. Raising the input plasma power resulted in higher yields of hydrogen from the non-thermal plasma processing of hexadecane. In addition, higher input plasma power raised the amount of cracking of the hexadecane volatiles. Non-thermal plasma processing of the furfural: hexadecane mixture also produced a low oxygen content product oil with a maximum yield of 11.32 wt% at 70 W input plasma power (Table 1). The synergistic interaction of the furfural and hexadecane with increasing plasma power resulting in a reduction in the higher molecular weight compounds and a consequent synergistic increase in the production of lighter hydrocarbons in the product oil.

4. Conclusions

In this study, furfural, as an oxygenated bio-oil model compound, was upgraded via deoxygenation in a non-thermal plasma process in the presence of hexadecane as a hydrogen donor to produce higher quality oil. Furfural and hexadecane were initially vaporised in a reactor and then processed in the non-thermal plasma reactor for cracking and autohydrogenation. The results indicate that non-thermal plasma aids in production of hydrogen *in-situ*, acting as a source for hydrogen during the process of hydrogenating furfural.

Increasing the input plasma power increased the feedstock conversion, gas yield and oil production. The highest gas and oil yields were achieved at 70 W input plasma power with a feedstock conversion of 20.46 wt %. Moreover, products yield and feed conversion synergies were positive at 70 W input power, confirming the interactions between furfural and hexadecane at high input plasma powers.

Increasing the input power during the non-thermal plasma process led to a decrease in the production of dual-oxygenated oil compounds produced from furfural and an increase in the proportion of light hydrocarbons produced from hexadecane. Non-thermal plasma processing of the mixture of furfural and hexadecane at higher input powers also reflected this trend by eliminating the production of dual-oxygenated compounds and heavy hydrocarbons in the product oil. The synergistic interaction between the furfural and hexadecane was positive, with higher percentage synergies occurring at higher input plasma powers. In contrast, the synergistic effect for most heavy hydrocarbons was negative, suppressing the formation of these compounds in the product oil, and this suppression increased with increasing power. This phenomenon could be attributed to the high-energy electrons in the non-thermal plasma environment colliding with the volatile components of the feedstock, thereby assisting in deoxygenation and the production of light hydrocarbons. The synergy results demonstrate the interaction between furfural and hexadecane, which intensified at higher input powers, resulting in a higher-quality oil with the introduction of both the non-thermal plasma reaction environment and a hydrogen donor feedstock.

CRediT authorship contribution statement

Maryam Khatibi: Writing – original draft, Methodology, Investigation. **Mohamad A. Nahil:** Methodology. **Paul T. Williams:** Writing – review & editing, Supervision, Funding acquisition.

Data availability

Data will be made available on request.

Acknowledgements

This work was supported by funding from the UK Engineering & Physical Sciences Research Council (EPSRC) SuperGen Bioenergy Hub (SGBHFF-May2021-06), which is gratefully acknowledged. Also, Maryam Khatibi, was awarded an EPSRC - University of Leeds scholarship to carry out the research, which again is gratefully acknowledged.

References

[1] J.W. Kim, H.W. Lee, I.-G. Lee, J.-K. Jeon, C. Ryu, S.H. Park, S.-C. Jung, Y.-K. Park, Influence of reaction conditions on bio-oil production from pyrolysis of construction waste wood, Renew. Energy 65 (2014) 41–48.

[2] R. Kumar, V. Strezov, Thermochemical production of bio-oil: a review of downstream processing technologies for bio-oil upgrading, production of hydrogen and high value-added products, Renew. Sustain. Energy Rev. 135 (2021) 110152.

[3] T.S. Ahamed, S. Anto, T. Mathimani, K. Brindhadevi, A. Pugazhendhi, Upgrading of bio-oil from thermochemical conversion of various biomass–Mechanism, challenges and opportunities, Fuel 287 (2021) 119329.

[4] J. Liu, X. Chen, W. Chen, M. Xia, Y. Chen, H. Chen, K. Zeng, H. Yang, Biomass pyrolysis mechanism for carbon-based high-value products, Proc. Combust. Inst. 39 (3) (2023) 3157–3181.

[5] H. Rönkkönen, K. Klemkaitė, A. Khinsky, A. Baltušnikas, P. Simell, M. Reinikainen, O. Krause, M. Niemelä, Thermal plasma-sprayed nickel catalysts in the clean-up of biomass gasification gas, Fuel 90 (3) (2011) 1076–1089.

[6] M. Artetxe, M.A. Nahil, M. Olazar, P.T. Williams, Steam reforming of phenol as biomass tar model compound over Ni/Al2O3 catalyst, Fuel 184 (2016) 629–636.

[7] A. Khosravanipour Mostafazadeh, O. Solomatnikova, P. Drogui, R.D. Tyagi, A review of recent research and developments in fast pyrolysis and bio-oil upgrading, Biomass conversion and biorefinery 8 (3) (2018) 739–773.

[8] M. Saidi, F. Samimi, D. Karimipourfard, T. Nimmanwudipong, B.C. Gates, M. R. Rahimpour, Upgrading of lignin-derived bio-oils by catalytic hydrodeoxygenation, Energy Environ. Sci. 7 (1) (2013) 13–129.

[9] T. Sundqvist, A. Oasmaa, A. Koskinen, Upgrading fast pyrolysis bio-oil quality by esterification and azeotropic water removal, Energy Fuel. 29 (4) (2015) 2527–2534.

[10] L. Ciddor, J.A. Bennett, J.A. Hunns, K. Wilson, A.F. Lee, Catalytic upgrading of bio-oils by esterification, J. Chem. Technol. Biotechnol. 90 (5) (2015) 780–795.

[11] S. Gupta, P. Mondal, V.B. Borugadda, A.K. Dalai, Advances in upgradation of pyrolysis bio-oil and biochar towards improvement in bio-refinery economics: a comprehensive review, Environ. Technol. Innovat. 21 (2021) 101276.

[12] H. Taghvaei, M.B. Hosseinzadeh, S. Rezazadeh, M.R. Rahimpour, A. Shariati, Upgrading of 4-methylanisole in a catalytic reactor with electric discharges: a novel approach to O-removal from bio-oils, Chem. Eng. J. 281 (2015) 227–235.

[13] H. Taghvaei, M.R. Rahimpour, Plasma upgrading of guaiacol as lignin pyrolytic-oil model compound through a combination of hydrogen production and hydrodeoxygenation reaction, J. Anal. Appl. Pyrol. 135 (2018) 422–430.

[14] C. Wang, Z. Guo, Y. Yang, J. Chang, A. Borgna, Hydrogenation of furfural as model reaction of bio-oil stabilization under mild conditions using multiwalled carbon nanotube (MWNT)- supported Pt catalysts, Ind. Eng. Chem. Res. 53 (2014) 11284–11291.

[15] P.A. Horne, P.T. Williams, Reaction of oxygenated biomass pyrolysis model compounds over a ZSM-5 catalyst, Renew. Energy 7 (2) (1996) 131–144.

[16] G. Lyu, S. Wu, H. Zhang, Estimation and comparison of bio-oil components from different pyrolysis conditions, Front. Energy 28 (2015) 1–11.

[17] S. Sitthisa, D.E. Resasco, Hydrodeoxygenation of furfural over supported metal catalysts: a comparative study of Cu, Pd and Ni, Catal. Lett. 141 (2011) 784–791.

[18] O. Sanahuja-Parejo, A. Veses, M. Navarro, J. López, R. Murillo, M. Callén, T. García, Drop-in biofuels from the co-pyrolysis of grape seeds and polystyrene, Chem. Eng. J. 377 (2019) 120246.

[19] M.V. Tsodikov, M.V. Chudakova, A.V. Chistyakov, Y.V. Maksimov, Catalytic conversion of cellulose into hydrocarbon fuel components, Petrol. Chem. 53 (2013) 367–373.

[20] A. Bogaerts, X. Tu, J.C. Whitehead, G. Centi, L. Lefferts, O. Guaitella, F.A. Jury, H. H. Kim, A.B. Murphy, W.F. Schneider, T. Nozaki, J.C. Hickes, A. Rousseau, F. Thevenet, A. Khacef, M. Carreon, The 2020 plasma catalysis roadmap, J. Phys. Appl. Phys. 53 (2020). #443001.

[21] P. Ghorbannezhad, S. Park, J.A. Onwudili, Co-pyrolysis of biomass and plastic waste over zeolite-and sodium-based catalysts for enhanced yields of hydrocarbon products, Waste Manag. 102 (2020) 909–918.

[22] L. Rodriguez-Luna, D. Bustos-Martinez, E. Valenzuela, Two-step pyrolysis for waste HDPE valorization, Process Saf. Environ. Protect. 149 (2021) 526–536.

[23] S.P. Tekade, P.P. Gugale, M.L. Gohil, S.H. Gharat, T. Patil, P.K. Chaudhari, D. S. Patle, A.N. Sawarkar, Pyrolysis of waste polyethylene under vacuum using zinc oxide, Energy Sources, Part A Recovery, Util. Environ. Eff. 1856976 (2020) 1–15.

[24] N. Al–Areqi, E. Alaghbari, A. Al–Alas, O. Saeed, H. Mufadhal, A. Al-Hatemi, Low–temperature and semi–batch production of liquid fuel comparable to commercial grade diesel by portland cement–catalyzed pyrolysis of waste polypropylene, American Journal of Applied and Industrial Chemistry 4 (2) (2020) 14–20.

[25] N. Hooshmand, M.R. Rahimpour, A. Jahanmiri, H. Taghvaei, M. Mohamadzadeh Shirazi, Hexadecane cracking in a hybrid catalytic pulsed dielectric barrier discharge plasma reactor, Ind. Eng. Chem. Res. 52 (12) (2013) 4443–4449.

[26] L. Wang, B. Sun, X. Zhu, Y. Xin, Z. Yan, Study on n-hexadecane cracking with introducing water by pulsed discharge in liquid, Fuel 293 (2021). #120400.

[27] M. Khatibi, M.A. Nahil, P.T. Williams, Improving the quality of bio-oil using the interaction of plastics and biomass through copyrolysis coupled with nonthermal plasma processing, Energy Fuel 38 (2) (2024) 1240–1257.

[28] F. Saleem, A. Abbas, A. Rehman, A.H. Khoja, S.R. Naqvi, M.Y. Arshad, K. Zhang, A. Harvey, Decomposition of benzene as a biomass gasification tar in CH_4 carrier gas using non-thermal plasma: parametric and kinetic study, J. Energy Inst. 102 (2022) 190–195.

[29] H.M. Nguyen, M.L. Carreon, Non-thermal plasma-assisted deconstruction of high-density polyethylene to hydrogen and light hydrocarbons over hollow ZSM-5 microspheres, ACS Sustain. Chem. Eng. 10 (29) (2022) 9480–9491.

[30] F. Saleem, A. Rehman, A. Abbas, A.H. Khoja, F. Ahmad, L. Liu, K. Zhang, A. Harvey, A comparison of the decomposition of biomass gasification tar compound in CO, CO_2, H_2 and N_2 carrier gases using non-thermal plasma, J. Energy Inst. 97 (2021) 161–168.

[31] H. Taghvaei, M.R. Rahimpour, Catalytic hydrodeoxygenation of bio-oil using in situ generated hydrogen in plasma reactor: effects of allumina supported catalysts and plasma parameters, Process Saf. Environ. Protect. 121 (2019) 221–228.

[32] S. Liu, D. Mei, M. Nahil, S. Gadkari, S. Gu, P. Williams, X. Tu, Hybrid plasma-catalytic steam reforming of toluene as a biomass tar model compound over Ni/Al_2O_3 catalysts, Fuel Process. Technol. 166 (2017) 269–275.

[33] M.R. Khani, S.H.R. Barzoki, M.S. Yaghmaee, S.I. Hosseini, M. Shariat, B. Shokri, A. R. Fakhari, S. Nojavan, H. Tabani, M. Ghaedian, Investigation of cracking by cylindrical dielectric barrier discharge reactor on the n-hexadecane as a model compound, IEEE Trans. Plasma Sci. 39 (9) (2011) 1807–1813.

[34] W. Chen, S. Shi, J. Zhang, M. Chen, X. Zhou, Co-pyrolysis of waste newspaper with high-density polyethylene: synergistic effect and oil characterization, Energy Convers. Manag. 112 (2016) 41–48.

[35] H. Yuan, H. Fan, R. Shan, M. He, J. Gu, Y. Chen, Study of synergistic effects during co-pyrolysis of cellulose and high-density polyethylene at various ratios, Energy Convers. Manag. 157 (2018) 517–526.

[36] M. Huang, L. Zhu, W. Zhang, L. Zhu, Z. Ma, D. Chen, Insight into the synergistic reaction mechanism of biomass pseudo components and low-density polyethylene for the production of light aromatics through co-catalytic fast pyrolysis over hierarchical HZSM-5, Fuel 324 (2022) 124699.

[37] F. Saleem, A.H. Khoja, J. Umer, F. Ahmad, S.Z. Abbas, K. Zhang, A. Harvey, Removal of benzene as a tar model compound from a gas mixture using non-thermal plasma dielectric barrier discharge reactor, J. Energy Inst. 96 (2021) 97–105.

[38] K. Sasujit, N. Homdoung, N. Tippayawong, Non-thermal plasma removal of naphthalene as tar model compound from biomass gasification, Energy Rep. 8 (2022) 97–103.

[39] U.H. Dahiru, F. Saleem, F.T. Al-sudani, K. Zhang, A.P. Harvey, Decomposition of benzene vapour using non-thermal plasmas: the effect of moisture content on eliminating solid residue, J. Environ. Chem. Eng. 10 (3) (2022) 107767.

[40] Y. Fan, D. Lu, Y. Han, J. Yang, C. Qian, B. Li, Production of light aromatics from biomass components co-pyrolyzed with polyethylene via non-thermal plasma synergistic upgrading, Energy 265 (2023) 126427.

[41] H. Hassan, B. Hameed, J. Lim, Co-pyrolysis of sugarcane bagasse and waste high-density polyethylene: synergistic effect and product distributions, Energy 191 (2020) 116545.

[42] F. Saleem, K. Zhang, A. Harvey, Temperature dependence of non-thermal plasma assisted hydrocracking of toluene to lower hydrocarbons in a dielectric barrier discharge reactor, Chem. Eng. J. 356 (2019) 1062–1069.

[43] W. Wang, Y. Ma, G. Chen, C. Quan, J. Yanik, N. Gao, X. Tu, Enhanced hydrogen production using a tandem biomass pyrolysis and plasma reforming process, Fuel Process. Technol. 234 (2022) 107333.

[44] E. Blanquet, M.A. Nahil, P.T.J.C.T. Williams, Enhanced Hydrogen-Rich Gas Production from Waste Biomass Using Pyrolysis with Non-thermal Plasma-Catalysis, 337, 2019, pp. 216–224.

[45] Z. Xu, N. Gao, Y. Ma, W. Wang, C. Quan, X. Tu, N. Miskolczi, Biomass volatiles reforming by integrated pyrolysis and plasma-catalysis system for H_2 production: understanding roles of temperature and catalyst, Energy Convers. Manag. 288 (2023) 117159.

[46] F. Meng, X. Li, H. Liang, G. Wang, L. Lu, J. Liu, Non-thermal plasma degradation of tar in gasification syngas, Chemical Engineering and Processing-Process Intensification 145 (2019) 107656.